Application of Artificial Neural Network and Predictor Screening Method for Downscaling Climatic Parameters

NAZAK ROUZEGARI
Department of Water Resources Engineering, Faculty of Civil Engineering
University of Tabriz
Tabriz
IRAN
nazak_rouzegari@yahoo.com
VAHID NOURANI
Department of Water Resources Engineering, Faculty of Civil Engineering
University of Tabriz
Tabriz
IRAN
&
Department of Water Resources Engineering, Faculty of Civil Engineering
Near East University
Nicosia
CYPRUS
v.nourani@yahoo.com
AMIR MOLAJOU
Department of Water Resources Engineering, Faculty of Civil Engineering
University of Science & Technology
Tehran
IRAN
amir.molaju3@yahoo.com

Abstract: - In this paper, artificial neural network (ANN) was used for downscaling the outputs of general circulation models (GCMs) to evaluate changes in precipitation and mean temperature for a future period in Urmia at the north-west of Iran. MIROC-ESM-CHEM from IPCC AR5 was selected as an acceptable model based on correlation coefficient (CC) values, which is calculated between precipitation of GCM models and precipitation data prepared by Urmia Meteorological Organization for 1951-2000. As a first step, the most important parameters of the MIROC-ESM-CHEM was selected before the downscaling process by ANN in the base period (1951-2000). Afterward, the future projections of precipitation and mean temperature during 2020–2060 were applied using ANN-based simulation according to the CC method. By comparing the results, the MIROC-ESM-CHEM showed a 2.01% increase under RCP4.5 and a 0.16% decrease under RCP8.5 in annual precipitation. Also, the temperature projection outputs showed the annual mean temperature would increase in the future period in this area, and it is likely to get warmer.

Key-Words: - ANN- Correlation coefficient-Climate change-Downscaling-GCM-Urmia

1 Introduction

Global climatic changes affected by carbon dioxide begin to appear within the next few decades. One of the most important effects of climate change is changing in water availability in different sections, such as agricultural productions, food control, municipal, and industrial. The precipitation and temperature are the most effective variables that studying their changes in the future can be more effective in increasing or omitting the negative impacts such as drought and flash floods. General circulation models (GCMs) have been developed to simulate the present climate and predict future climatic change and investigate future precipitation and temperature fluctuations [1]. The relationships between synoptic-scale circulation and the local

climate must be well understood to predict precipitation and temperature at the regional scale [2]. This should be followed by the application of downscaling procedures. Statistical downscaling methods are the most largely used in predicting hydrologic impact studies under climate change scenarios [3]. Several statistical downscaling methods have been already developed and used for the statistically downscaling of GCM outputs. In the recent decade, artificial intelligence (AI)-based methods such as ANN have been successfully used to predict the hydro-climatic variables or downscaling GCM outputs [4], [5], [6]. There are plenty of GCM data, and the huge numbers of inputs to the ANN model leads to poor performance of the model, so selecting the dominant inputs among many potential input variables is unavoidable [7], [8], [9], [10].

This study shows the results of the CC method as a feature extraction method in the statistical downscaling of precipitation and mean temperature at Urmia synoptic station. Finally, the future climate is projected based on the CC feature extraction method and appropriate downscaling model of GCM (i.e., MIROC-ESM-CHEM) under RCP4.5 and RCP8.5 scenarios.

2 Methods and materials

2.1 Case Study

Urmia city (37° 55′ N, 45° 08′ E) is located in the west of Urmia Lake in the north-west of Iran (Fig.1). The city is affected by the winds of the northern and Siberian, Atlantic Ocean, and black and Mediterranean seas. It is an area with a cold and semi-arid climate. The average annual precipitation in this place is about 338 mm, and the average number of ice days during a year is 120 days. The years 1951–2000 were selected as the base period in this study. Monthly precipitation and mean temperature data are available for the base period. Figs.2 and 3 shows the distribution of monthly precipitation and mean temperature of the Urmia synoptic station during 1951–2000, respectively.

2.2 CC Method

The CC is a common method to evaluate the linear relation between two variables with the value in –1 to +1 range, in which +1 indicates the strong positive linear association and −1 shows the strong negative linear relationship. The value of zero indicates no relationship between the two variables. CC is defined as Eq. 1 [11]:

$$CC = \frac{\sum(X-\bar{X})\sum(Y-\bar{\bar{Y}})}{\sqrt{\sum(X-\bar{X})^2\sum(Y-\bar{Y})^2}} \quad (1)$$

Where X and Y indicate predictand and predictor, and $\bar{X}$ and $\bar{Y}$ are mean values of predictand and predictor, respectively.

2.3 ANN Model

In this paper, the three-layer Feed-Forward Neural Network (FFNN) structure is used to downscale the GCM outputs. The Levenberg-Marquardt scheme of the backpropagation algorithm, which has a higher convergence rate [12], was applied in the ANN training process to achieve the best efficiency of the ANN model. The activation function that was applied as the nonlinear kernel of neural networks is the sigmoid Tangent function. The process of network training was stopped when the error rate was obtained in the verification data. In this kind of model, especially in the ANN model, the developing of the appropriate architecture (i.e. the number of hidden neurons and the number of iteration) is such an important subject that should be taken into consideration [10]. The best conditions were obtained by trial-error testing.

2.4 Evaluation Criteria

In this study, both testing and training performances were evaluated using the following indices [13]:

1. RMSE that indicates the error in the units of the model's output.

$$RMSE = \sqrt{\frac{1}{n}\sum_{i=1}^{n}(X-Y)^2} \quad (2)$$

2. The correlation coefficient (r) that indicates how well the model can replicate the observed data. It ranges from 0 to 1.0 and 1.0 is the perfect match.

$$r = \frac{\sum_{i=1}^{n}(X_i-\bar{X})(Y_i-\bar{Y})}{[\sum_{i=1}^{n}(X_i-\bar{X})^2]^{0.5}[\sum_{i=1}^{n}(Y_i-\bar{Y})^2]^{0.5}} \quad (3)$$

Here X and Y are observed and simulated data, respectively.

3 Results and Discussion

In this study, the predictors (i.e. precipitation) of 22 GCMs model from the 5th Assessment Report (AR5) of IPCC (CMIP5) were chosen. Among 22 GCMs, one GCM model was selected by comparing CC over monthly precipitation (predictor) data of GCMs and precipitation data (predictand) prepared by the Urmia Meteorological Organization for 1951-2000.

The predictors were picked out in four grid points around the study area. The results are shown in Table 1. It can be inferred that the MIROC-ESM-CHEM model with a higher value of CC (i.e., equal to 0.57) is the best in this study. The applied predictors in the MIROC-ESM-CHEM model were selected as the previous study [14]. In the downscaling procedure, it is important to select the dominant predictors [15]. So for this purpose, the CC feature extraction method was applied. In this way, the predictors with the maximum values of CC, computed between predictor and predictand, in each grid point were ranked and selected. Table 2 presents the dominant predictors of the MIROC-ESM-CHEM model. In this table "a" indicates the number of grid point selected around the city based on MIROC-ESM-CHEM model (a=1, 2, 3, 4). The results of precipitation in Table 2 denote that the precipitation depends on the atmosphere mass content of cloud ice. This water and ice crystals (clivi) can fall due to the gravity and cause to rain. Another parameter is Toa outgoing longwave flux. The solar radiation on Earth (rlut) heats its air. This air can rise (ta (200)) and expand and get cooler. Also, the variables from the humidity type (i.e. hur (700), hur (200)) are other dominant parameters that were expected to be chosen because of the obvious and important role of humidity in precipitation formation [14]. Similar to the case of precipitation, the linear relation of mean temperature with the temperature of large scale variables was calculated. So, the air temperature (ta), the sea surface temperature (ts) and the near-surface air temperature (tas) in different grid points were selected as dominant predictors in the CC-based method.

In the next step, the dominant predictors extracted by the CC feature extraction method were downscaled by the ANN model for Urmia city during the base period (1951-2000). For this purpose, 75% of data were selected for training, and 25% of data were selected for testing [16]. 50-year average monthly precipitation and temperature downscaled from MIROC-ESM-CHEM model predictions were compared to the 50-year average monthly observed precipitation and temperature in Figs.4 and 5 for the base period, respectively. As shown in these figures, the MIROC-ESM-CHEM model has predicted the average precipitation that is 5.45% greater than observed precipitation, and the average temperature that is 0.9% higher than the observed temperature in several months. The results of precipitation and temperature downscaling according to the r and RMSE evaluation criteria are presented in Table 3. It can be seen that the MIROC-ESM-CHEM model produces acceptable climate prediction for this research.

In the final step, the monthly precipitation and mean temperature of Urmia city were projected for the future period (2020–2060) for MIROC-ESM-CHEM, which are shown in Figs.6 and 7, respectively. The future climate variables for this model were extracted under RCP4.5 and RCP8.5 scenarios in four mentioned grid points. According to Fig.6, the precipitation will both increase and decrease in some months during 2020-2060. It can be seen that the precipitation will increase during summer based on both scenarios, and the results are distinct in other months. Generally, the amount of precipitation increases by 2.01% under RCP4.5 and decreases 0.16% under RCP8.5 relative to the base period. The results of the mean temperature indicate that the mean temperature will increase in the future (see Fig.7); however, it will be almost constant in May, July, and October based on RCP8.5 scenarios. By calculating the change percentage for the mean temperature, it is obvious that future periods exhibit a higher temperature of about 3.66% and 3.3% under RCP4.5 and RCP8.5, respectively, in comparison with the base period. Generally, it can be said that the increase of global warming in the future could lead to increasing the sea level and the amount of humidity, which will affect the precipitation pattern.

4 Conclusion

In this study, the impacts of climate change on the monthly precipitation and mean temperature values of Urmia city were investigated between the years 2020 and 2060. For this purpose, the data of the GCM model (i.e., MIROC-ESM-CHEM) under CMIP5 scenarios (i.e., RCP4.5 and RCP8.5) were applied for downscaling the monthly precipitation and mean temperature using the ANN model. The CC feature extraction method was used to determinate the dominant variables in the region, which improved the results of the downscaling model. The results indicate that, according to outcomes, it is expected that the monthly precipitation of the study area will change -0.16 – 2.01%, while the mean temperature will increase between 3.3– 3.66%. It is obvious that the increase of global warming in the future could lead to a change in sea level, the amount of humidity, and the precipitation pattern.

References:

[1] Xu, Chong-yu, From GCMs to River Flow: A Review of Downscaling Methods and

Hydrologic Modelling Approaches, *Journal of Progress in physical Geography,* Vol.23, No.2, 1999, pp. 229-249.

[2] Schoof, Justin T., and S. C. Pryor, Downscaling Temperature and Precipitation: A Comparison of Regression□Based Methods and Artificial Neural Networks, *International Journal of Climatology: A Journal of the Royal Meteorological Society,* Vol.21, No.7, 2001, pp. 773-790.

[3] Khan Mohammad Sajjad, Paulin Coulibaly, and Yonas Dibike, Uncertainty Analysis of Statistical Downscaling Methods, *Journal of Hydrology,* Vol.319, No.1-4, 2006, pp. 357-382.

[4] Harpham Colin, and Robert L. Wilby, Multi-Site Downscaling of Heavy Daily Precipitation Occurrence and Amounts, *Journal of Hydrology,* Vol.312, No.1-4, 2005, pp. 235-255.

[5] Chadwick, R., Coppola, E., & Giorgi, F. An Artificial Neural Network Technique for Downscaling GCM Outputs to RCM Spatial Scale, *Journal of Nonlinear Processes in Geophysics,* Vol.18, No.6, 2011, pp. 1013–1028.

[6] Su, Buda, Xiaofan Zeng, Jianqing Zhai, Yanjun Wang, and Xiucang Li, Projected Precipitation and Streamflow under SRES and RCP Emission Scenarios in the Songhuajiang River Basin, China, *Journal of Quaternary international,* Vol.380, 2015, pp. 95-105.

[7] Sachindra, D. A., Huang, F., Barton, A., and Perera, B. J. C, Least Square Support Vector and Multi□Linear Regression for Statistically Downscaling General Circulation Model Outputs to Catchment Streamflows, *International Journal of Climatology,* Vol.33, No.5, 2013, pp. 1087-1106.

[8] Ahmadi, Mohsen, Omid Bozorg Haddad, and Hugo A. Loáiciga, Adaptive Reservoir Operation Rules Under Climatic Change, *Journal of Water Resources Management,* Vol.29, No.4, 2015, pp. 1247-1266.

[9] Taormina, Riccardo, Kwok-Wing Chau, and Bellie Sivakumar, Neural Network River Forecasting Through Base Flow Separation and Binary-Coded Swarm Optimization, *Journal of Hydrology,* Vol.529, 2015, pp. 1788-1797.

[10] Nourani, V., Razzaghzadeh, Z., Baghanam, A. H., and Molajou, A, ANN-Based Statistical Downscaling of Climatic Parameters Using Decision Tree Predictor Screening Method, *Journal of Theoretical and Applied Climatology,* Vol.137, No.3-4, 2019, pp. 1729-1746.

[11] Baghanam, Aida Hosseini, Vahid Nourani, Mohammad-Ali Keynejad, Hassan Taghipour, and Mohammad-Taghi Alami, Conjunction of Wavelet-Entropy and SOM Clustering for Multi-GCM Statistical Downscaling, *Journal of Hydrology Research,* Vol.50, No.1, 2019, pp. 1-23.

[12] Kisi, Özgür, Multi-Layer Perceptrons with Levenberg-Marquardt Training Algorithm for Suspended Sediment Concentration Prediction and Estimation, *Journal of Hydrological Sciences,* Vol.49, No.6, 2004, pp. 1025–1040.

[13] Babel, M. S., T. A. J. G. Sirisena, and N. Singhrattna, Incorporating Large-Scale Atmospheric Variables in Long-Term Seasonal Rainfall Forecasting Using Artificial Neural Networks: An Application to The Ping Basin in Thailand, *Journal of Hydrology Research,* Vol.48, No.3, 2017, pp. 867-882.

[14] Jato-Espino, D., Sillanpää, N., Charlesworth, S. M., & Rodriguez-Hernandez, J., A Simulation-Optimization Methodology to Model Urban Catchments Under Non-Stationary Extreme Rainfall Events, *Journal of Environmental Modelling & Software,* 2017.

[15] Kisi, Ozgur, Evapotranspiration Modelling from Climatic Data Using a Neural Computing Technique, *Journal of Hydrological Processes, An International Journal,* Vol.21, No.14, 2007, pp. 1925-1934.

[16] Komasi, Mehdi, and Soroush Sharghi, Hybrid Wavelet-Support Vector Machine Approach for Modelling Rainfall–Runoff Process, *Journal of Water Science and Technology,* Vol.73, No.8, 2016, pp. 1937-1953.

Appendix 1

Fig.1 Geographical location of the study area

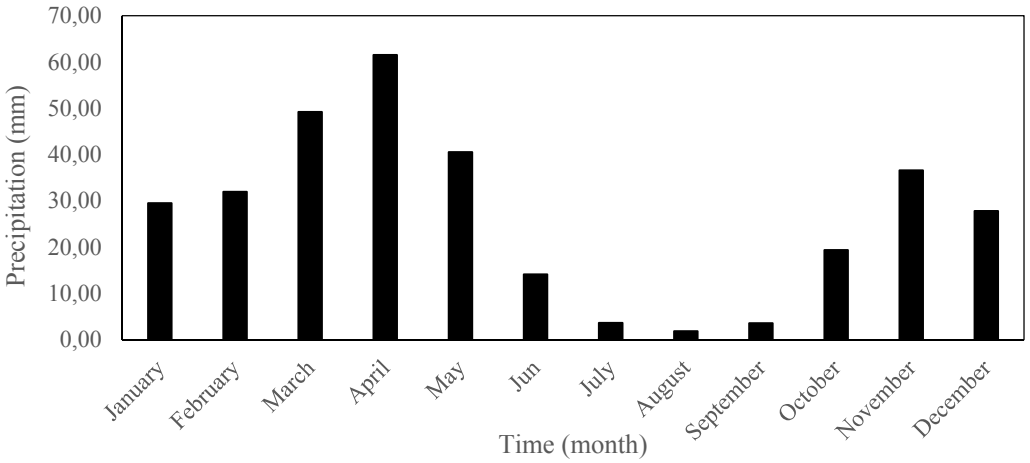

Fig. 2 Urmia monthly precipitation (1951-2000)

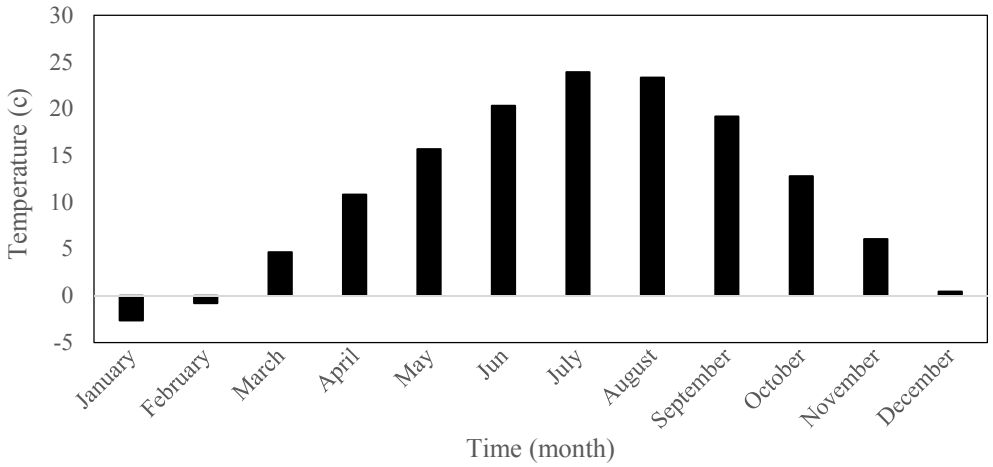

Fig. 3 Urmia monthly temperature (1951-2000)

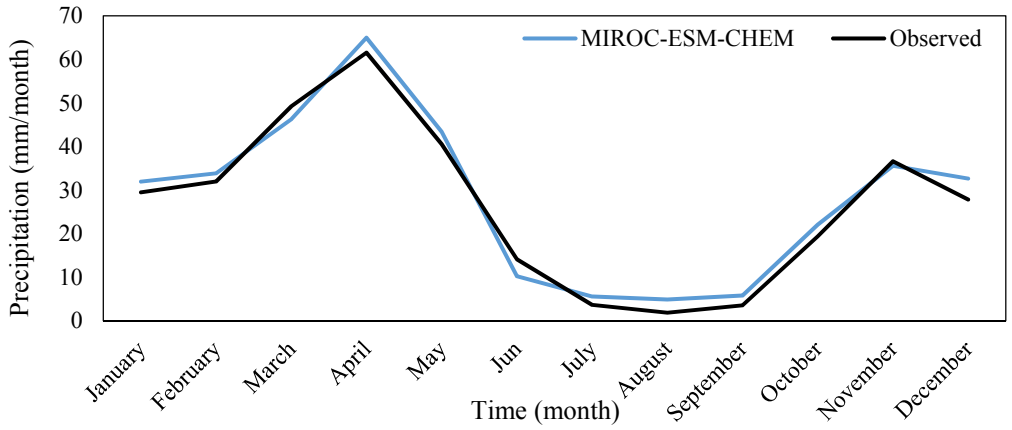

Fig. 4 Observed and simulated precipitation values for the base period (1951–2000) based on MIROC-ESM-CHEM and ANN model.

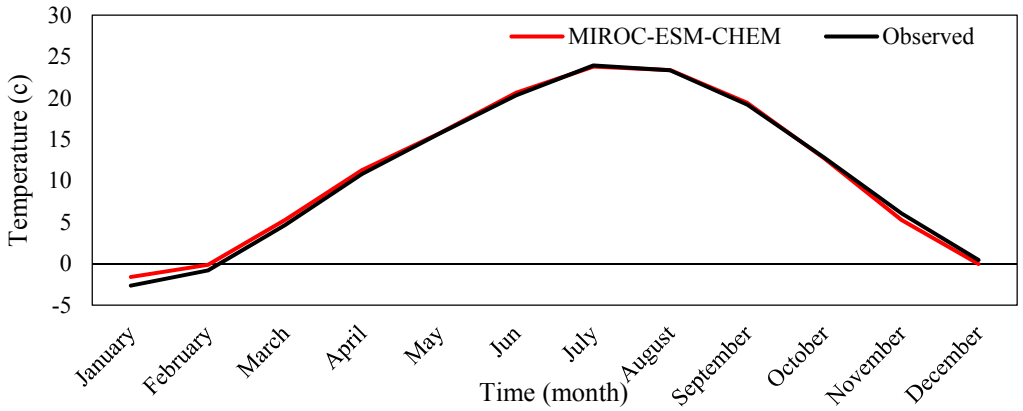

Fig. 5 Observed and simulated temperature values for the base period (1951–2000) based on MIROC-ESM-CHEM and ANN model.

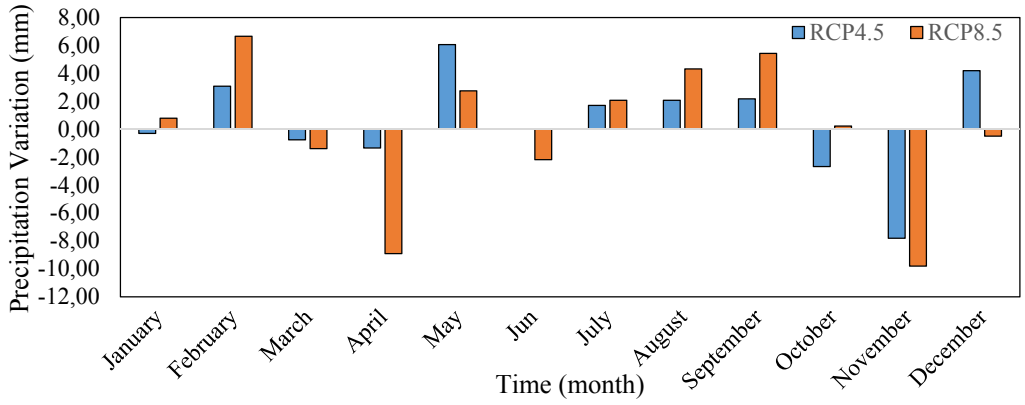

Fig. 6 Monthly precipitation variation according to projected and baseline

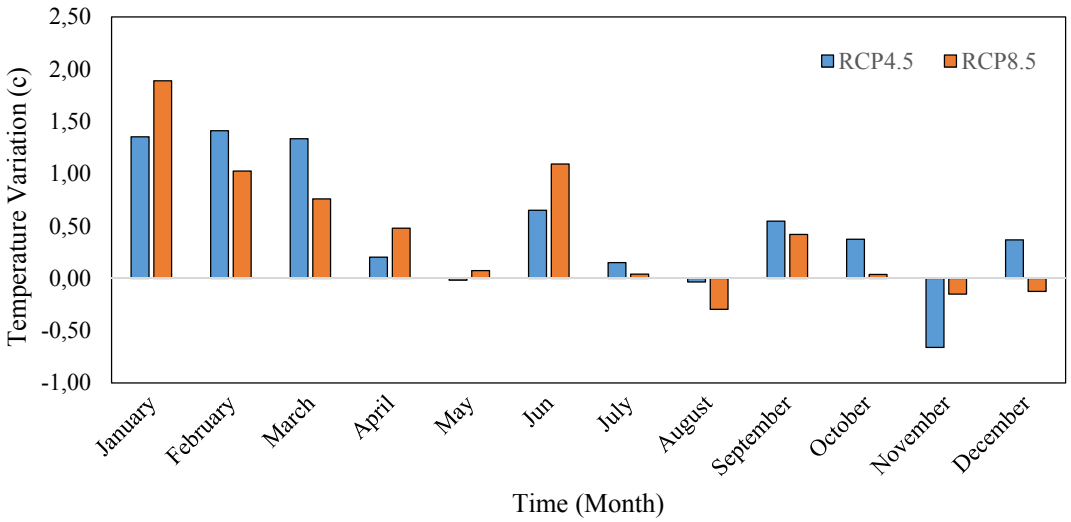

Fig. 7 Monthly temperature variation according to projected and baseline

Appendix 2

Table 1 Appropriate GCM model based on CC method

	AR5				
	GCM model	**S1**	**S2**	**S3**	**S4**
1	BCC-CSM 1-1-m	0.18	0.22	0.12	0.15
2	BNU-ESM	0.13	0.14	0.13	0.14
3	CanESM2	0.27	0.24	0.23	0.19
4	CCSM4	0.29	0.32	0.24	0.27
5	CMCC-CMS	0.38	0.34	0.28	0.37
6	CSIRO-Mk3-6-0	0.29	0.21	0.14	0.20
7	EC-EARTH	0.40	0.38	0.41	0.42
8	FGOALS-g2	-0.25	-0.22	-0.25	-0.22
9	FIO-ESM	0.28	0.28	0.28	0.28
10	**MIROC-ESM-CHEM**	**0.43**	**0.57**	**0.43**	**0.44**
11	MPI-ESM-MR	0.40	0.23	0.29	0.38
12	MRI-CGCM3	0.38	0.38	0.26	0.33
13	ACCESS1-3	0.17	0.21	0.41	0.28
14	CESM1-BGC	0.34	0.32	0.28	0.33
15	CMCC-CM	0.39	0.38	0.36	0.38
16	CNRM-CM5	0.31	0.29	0.31	0.29
17	GFDL-CM3	0.32	0.33	0.28	0.40
18	GISS-E2-H	0.24	0.03	0.34	0.37
19	INMCM4	0.28	0.28	0.21	0.24
20	IPSL-CM5A-LR	0.25	0.04	0.16	0.16
21	MIROC5	0.29	0.29	0.20	0.23
22	NorESM1-M	0.36	0.35	0.23	0.26

Table 2 The selected dominant predictors based on CC method

Model	Dominant predictors for precipitation[(a)]	Dominant predictors for temperature[(a)]
MIROC-ESM-CHEM	hur(700)(1), ta(200)(1), rlut(1), hur(700)(2), clivi(2)	ta(850)(1), tas(2), ts(2), tas(3), ts(3), ta(850)(3)

Table 3 The results of downscaling by ANN model using dominant CC feature extraction method (1951-2000)

Climate variable	r		RMSE	
	Train	Test	Train	Test
Precipitation	0.88	0.84	0.11	0.14
Temperature	0.98	0.97	0.05	0.06